



Autoclave sterilization of an in-house 3D-printed polylactic acid piece: biological safety and heat-induced deformation

Joan Ferràs-Tarragó¹ · Oihana Sabalza-Baztán² · Jose Miguel Sahuquillo-Arce² · Manuel Ángel Angulo-Sánchez¹ · Carolina De-La-Calva Ceinos¹ · Jose Vicente Amaya-Valero¹ · Francisco Baixauli-García¹

Received: 11 February 2021 / Accepted: 12 April 2021 / Published online: 6 May 2021
© Springer-Verlag GmbH Germany, part of Springer Nature 2021

Abstract

Aims Fused filament fabrication 3D printing with polylactic acid filaments is the most widely used method to generate biomodels at hospitals throughout the world. The main limitation of this manufacturing system is related to the biomodels' temperature sensitivity, which all but prevents them to be sterilized using conventional methods. The purpose of this study is to define an autoclave temperature-resistant FFF-PLA 3D printing protocol to print 3D fractures biomodels during pre-operative planning.

Methods and results Six different printing protocols were established, each with a different infill percentage. Ten distal radius biomodels were printed with each protocol and each biomodel was subject to 3D scanning. The biomodels were subsequently autoclave-sterilized at 134 °C and subjected to a new scanning process, which was followed by a calculation of changes in area, volume and deformity using the Hausdorff–Besicovitch method. Finally, 192 polylactic acid models were produced using the printing protocol offering the greatest resistance and were contaminated with 31 common nosocomial pathogens to evaluate the effectiveness of sterilizing the model printed using the said protocol. Sterilization resulted in a mean deformation of the biomodel of 0.14 mm, a maximum deformity of 0.75 mm, and a 1% area and a 3.6% volume reduction. Sterilization of the pieces printed using the analyzed protocol was 100% effective.

Conclusions The analyzed 3D printing protocol may be applied with any FFF-PLA 3D printer, it is safe and does not significantly alter the morphology of biomodels. These results indicate that 3D printing is associated with significant advantages for health centers as it increases their autonomy, allowing them to easily produce 3D biomodels that can be used for the treatment of fractures.

Keywords 3D printing · Custom made models · Polylactic acid sterilization

Introduction

The use of 3D printing as an aid to preoperative planning is one of the major developments of the last decade in the field of orthopedic and trauma surgery [1–4]. Its advantages

include reductions in OR time, easy identification of the center of rotation of orthopedic deformities, less frequent use of intraoperative fluoroscopy, decreases in bleeding, more efficient fracture reduction, and shorter bony union

✉ Joan Ferràs-Tarragó
cotferras@gmail.com

Oihana Sabalza-Baztán
oisa1992b@gmail.com

Jose Miguel Sahuquillo-Arce
wadjur@hotmail.com

Manuel Ángel Angulo-Sánchez
mangulosa@hotmail.com

Carolina De-La-Calva Ceinos
carolinadelacalva@gmail.com

Jose Vicente Amaya-Valero
joseamayacot@gmail.com

Francisco Baixauli-García
baixauli_fragar@gva.es

¹ Orthopaedic Surgery and Traumatology, Hospital La Fe, Av Fernando Abril Martorell 106, Valencia, Spain

² Microbiology, Hospital La Fe, Av Fernando Abril Martorell 106, Valencia, Spain

time. In addition, 3D printing has been hailed as a highly cost-effective technology [5–10].

For all these reasons, 3D printing is nowadays the subject of a large number of articles in the orthopedic and trauma surgery literature [1, 2]. The manufacturing of biomodels and custom-made guides is currently the main use of this technology, accounting for 83% of publications related to 3D printing [1].

Of all the 3D printers available in the market, those incorporating fused filament fabrication (FFF) technology and poly-lactic acid (PLA) filaments are the most widespread. These printers are easy to use, safe, economical, reliable and can be used by any hospital as they do not generate waste or require a dedicated facility [11–15].

The main limitation of FFF technology is related to the sterilization of biomodels after they are printed. PLA is a heat-sensitive thermoplastic material. Use of low-temperature sterilization with ethylene oxide or vaporized hydrogen peroxide, required for biomodels incorporating this technology, is much slower and not as affordable to many hospitals, which has restricted the use of the technology [16, 17]. Moreover, chemical sterilization induces physical and chemical changes in PLA, which could result in alterations to the structure and composition of biomodels [18, 19]. Studies published on the use of chemical disinfectants do not consider these changes, which means that such agents must be used with care when sterilizing biomodels [20].

The purpose of the present study is to evaluate the biological safety of autoclave sterilization in models printed with FFF-PLA technology as well as the autoclaving-induced deformation of the biomodels.

Methods

Evaluation of the effects of sterilization on the morphology of biomodels

Manufacture of biomodels

A constant printing protocol was defined (Table 1). Six different 3D printing protocols were established, which only differed with respect to their infill percentage: Infill percentages ranged from 5% in group 1A to 30% in group 1F (the infill percentage in the in-between groups increased progressively in 5% intervals). Ten PLA distal radius biomodels were printed using each protocol (Table 1). They were obtained from a CT-scan of a patient with an intact distal radius (3D Slicer® Harvard Medical School, MA, USA). The modeling was carried out using MeshMixer software (Autodesk, CA, USA). The printing parameters were defined using Cura software.

Table 1 Description of the groups, including infill data and the printing time and PLA filament weight increases resulting from growing infill percentages

Parameter	Infill percentage	Printing time (min)	PLA filament grams
GROUP 1A	5%	324	50
GROUP 1B	10%	361	57
GROUP 1C	15%	400	66
GROUP 1D	20%	437	74
GROUP 1E	25%	516	82
GROUP 1F	30%	564	90

Printing time and PLA filament weight data refer to the 10 biomodels produced with each printing protocol. The images show the internal structure differences between group 1A (A) and group 1F (B)

To determine the effects of autoclaving on the morphology of biomodels, each biomodel was individually scanned prior to being sterilized by 3D scanning (SOL 3D Scanner, Scan Dimension® Svanevang, Denmark). Subsequently, they were all sterilized in an individual package and, finally, subjected to a new scanning process. 3D models were saved in stereolithography file format (.stl) before and after sterilization to analyze whether sterilization produced any changes in their morphology. Morphological alterations were analyzed based on four parameters: mean deformation across the whole area, maximum deformation, changes in the area and changes in volume (Fig. 1, green arrow).

The Hausdorff–Besicovitch method was used to evaluate the mean and the maximum deformation following a manual alignment process (MeshLab, Autodesk, CA, USA) [21], based on a protocol previously described in the literature [9, 22].

Changes related to the area and volume of the biomodels were calculated before and after sterilization using Netfabb software (Autodesk, CA, USA); the differences between the values were calculated.

Errors calculated using this procedure include both errors secondary to autoclaving-induced deformation and errors occurred during model alignment. A constant printing and scanning error was allowed for all biomodels. To identify errors during the manipulation of biomodels, ten pieces were obtained from group 1 (5% infill) and scanned twice prior to sterilization (Fig. 1, blue arrow). Morphological discrepancies were calculated using the same method. As it was the same piece, any differences were attributed to an error related to the alignment of the biomodels. This value was taken as the minimal expected error between the biomodels before and after sterilization. It was a controlled method-related error rather than a deformity resulting from the sterilization process.

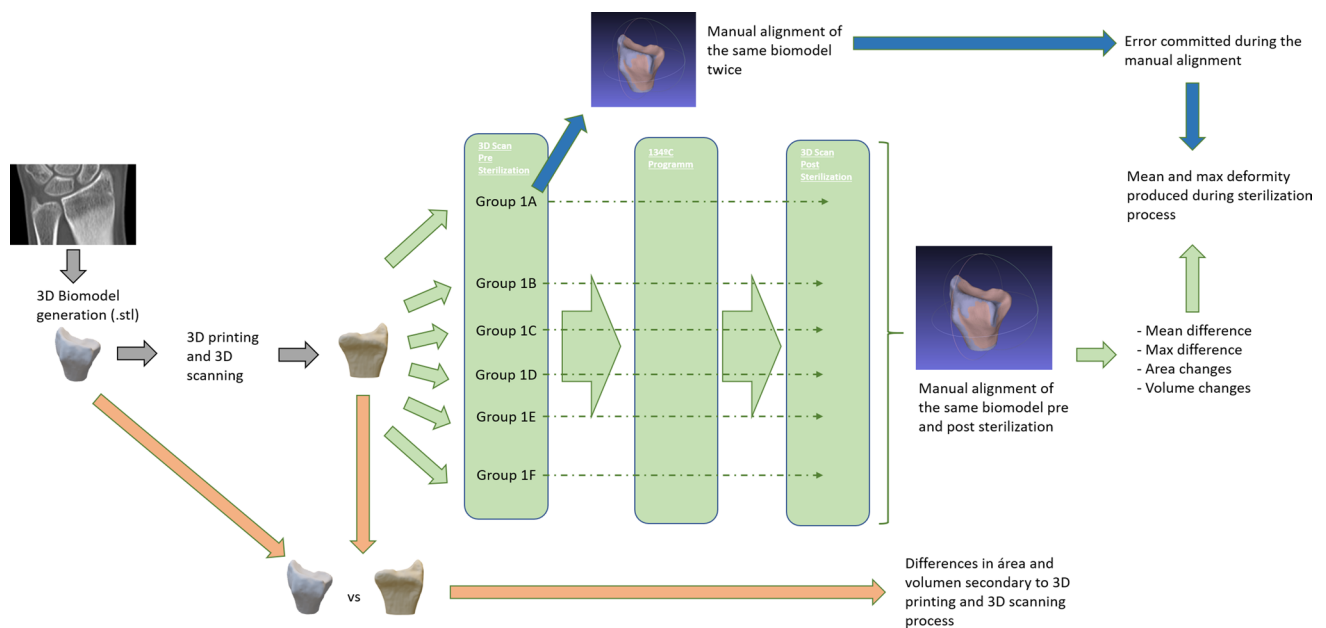


Fig. 1 Explanatory diagram of the methodology used to analyze the effects of autoclaving on the morphology of the biomodel. The orange arrows show the route followed to analyze errors associated with 3D printing and scanning. The green arrows show the route followed to analyze overall deformation following autoclaving. The blue arrows show the route followed to analyze the errors occurred during

manual alignment. Manual alignment shows that biomodel alignment follows a constant protocol across all comparisons. Automatic alignment systems are faster but do not provide any insights into the protocol followed to achieve the alignment, which could lead to misleading results

Errors occurring during 3D printing and scanning were evaluated jointly by comparing the area and the volume of the .stl file obtained from the CT-scan and the .stl file obtained after printing and scanning the biomodels prior to sterilization (Fig. 1, orange arrow).

Sample sterilization

A total of 192 rectangular models (40 mm × 8 mm × 3 mm, Audoesk Fusion 360[®]) were designed and printed using the FFF-PLA system (Eryone Filament PLA White[®]) with the parameters defined in Table 2 and with an infill percentage of 30%, which was the highest infill percentage used in our study (Cura Ultimaker[®], Utrecht, The Netherlands).

A total of 31 nosocomial pathogens commonly found in internal fixation hardware were selected. They included both gram positive [—Methicillin-resistant *Staphylococcus aureus* (3 strains), *Staphylococcus capitis* (2 strains), *Staphylococcus hominis* (3 strains), *Staphylococcus pasteurii* (1 strain) (3 strains), *Corynebacterium striatum* (2 strains), *Corynebacterium jeikeium* (1 strain), *Enterococcus faecium* (2 strains), *Enterococcus faecalis* (2 strains), and *Cutibacterium acnes* (2 strains)] and gram negative [*Pseudomonas aeruginosa* (2 strains) and fungi (—*Candida albicans* (2 strains), *Candida tropicalis* (1 strain), *Candida glabrata* (2 strains), *Candida parapsilosis* (1 strain) and *Candida auris* (2 strains)] organisms.

Table 2 Description of the printing parameters defined in the protocol

Parameter	Value
Layer height	0.3 mm
Wall thickness	0.8 mm
Wall line count	2
Top/bottom thickness	1.1 mm
Top/bottom layers	4
Nozzle diameter	0.4 mm
Temperature	220 °C
Print speed	50 mm/s
Horizontal expansión	0 mm
Infill density	5%–10%–15%– 20%–25%– 30%
Infill pattern	Gyroid

The infill percentage was progressively increased in 5% increments. The printer used was Ender 3 (Creality, Shenzhen, China)

All pathogens were obtained at the hospital and subsequently thawed, cultured in plates with the necessary growth media, and identified by MALDI-TOF mass spectrometry (VITEK[®]MS, bioMérieux, Durham, NC).

The sterilization process was evaluated by inoculating three PLA pieces in monomicrobial cultures containing the stated microorganisms. The cultures were performed in Trip-tisoja liquid medium (TSB; Biónica Diagnósticos SL). In

total, 186 PLA plates and 6 negative controls with pathogens were cultured (Fig. 2).

After a 10 day-long culture, PLA plates were randomized into 3 groups: 2A, 2B and 2C (Fig. 2). Group 2A underwent sterilization using an autoclave program at 134 °C (2.1 bar, 8 min' vacuum time, 12 min' sterilization time and 10 min' drying time). To evaluate the viability of the pathogen and absence of contamination, plates in group 2B were cultured in different culture media: Aerobic Columbia Agar (BD Columbia Agar with 5% SheepBlood[®]), Columbia Anaerobic Agar, and Sabouraud Agar (BBL Sabouraud Dextrose Agar[®]). Group 2C was used to make crystal violet stains on the biofilms formed on the PLA.

Once sterilization was achieved, new cultures were performed in a TSB medium. Culture results were monitored continuously from the first 24 h until the end of a 12 months period. The result was expressed in terms of a sterilization success rate (Fig. 2).

Statistical analysis

Volume, area, and deformity-related differences during the sterilization process were subjected to statistical hypothesis

testing by performing a Student's *t* test for paired data when values were normally distributed and a Wilcoxon test when they were distributed non-normally.

When comparing values between groups, Student's *t* test was used for independent data when data distribution was normal; the Mann–Whitney *U* test was used for non-normal data distributions.

Normality in data distribution was analyzed using the Saphiro–Wilk test; distribution was considered normal when *p* value was > 0.05.

The R statistics software (R Project[®]) was used for the statistical analysis with differences being considered statistically significant when $\alpha = 0.01$.

The study was approved by the hospital's ethical committee.

Results

Group 1E (25% infill) was the printing protocol showing the highest efficiency with respect to autoclave-sterilization, with a mean deformity of 0.41 mm (SD 0.09 95% CI 0.34–0.47, *p* value < 0.01). Group 1F (30% infill) exhibited

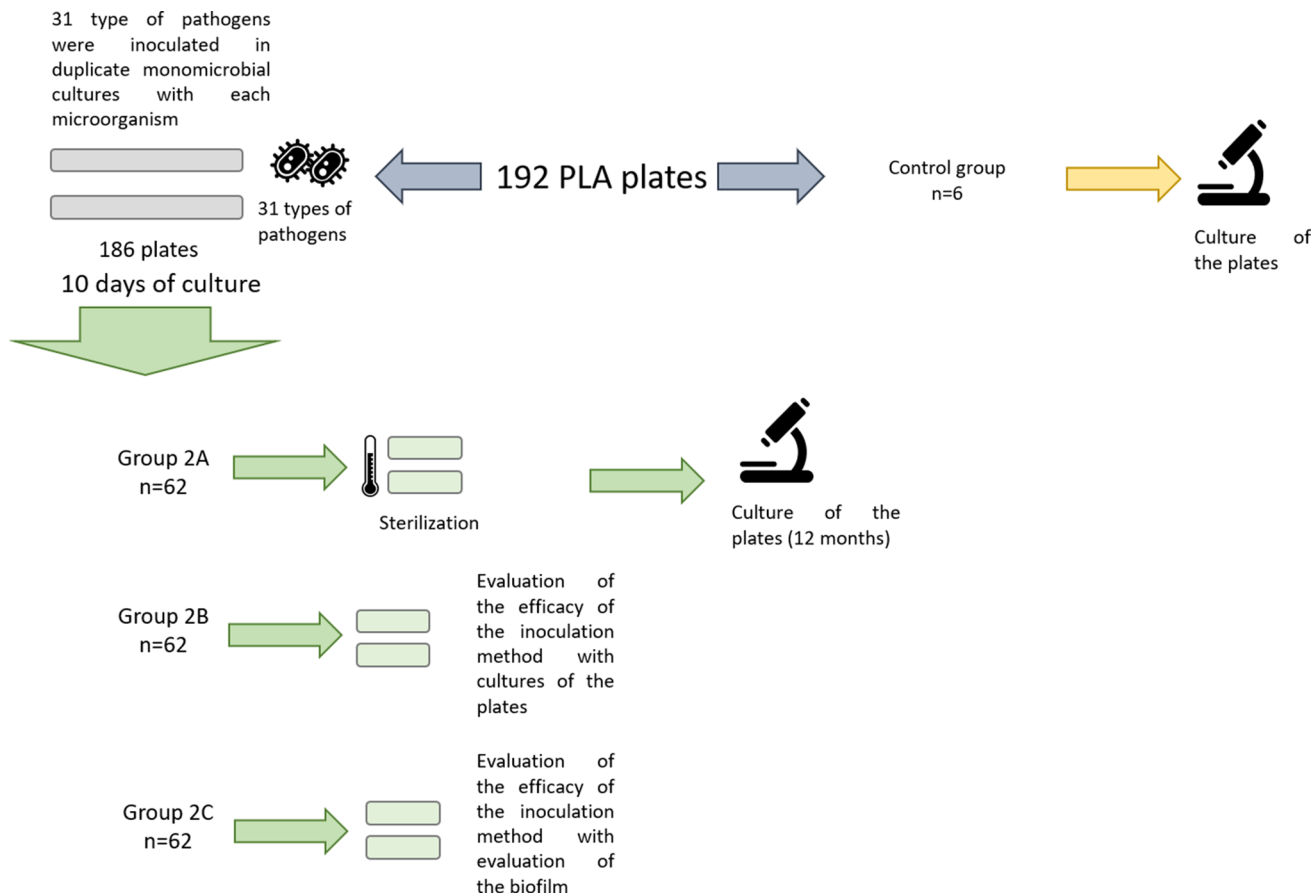


Fig. 2 Diagram showing the methodology used to evaluate the effectiveness of autoclaving for sterilizing 3D biomodels

0.02 mm less deformation on average, with a final mean deformation of 0.39 mm (SD 0.08 95% CI 0.33–0.45, *p* value < 0.01). The mean deformation difference between groups 1E and 1F was not statistically significant (*p* value = 0.7, 95% CI – 0.06–0.09), nor were the maximum deformation differences between groups 1E and 1F, with a mean difference of 0.16 mm [95% CI – 0.73–(0.42) *p* value = 0.56] (Figs. 3, 4).

Differences related to mean and maximum error between groups 1D and 1E were statistically significant (*p* value < 0.01), as were the differences between the rest of the groups (Figs. 3, 4).

The deformity observed in the printing protocols with infill percentages of 20% or less was significantly greater than that observed in higher infill percentages. The greatest deformities were observed in group 1A, with a mean deformity of 1.72 mm and a maximum deformity of 6.21 mm (Fig. 3).

The mean error attributable to image manipulation was 0.27 mm (SD 0.12 mm 95% CI 0.18–0.36 *p* value < 0.01). The maximum error attributable to image manipulation was 0.9 mm (SD 0.42 95% CI 0.59–1.2 *p* value < 0.01) (Figs. 3, 4).

Sterilization brought about a reduction in the total area of biomodels. The smallest area loss was observed in group 1E, with a mean area loss of 0.29 cm² (SD 0.83), which resulted in a non statistically significant difference between pre- and post-sterilization volumes (*p* value = 0.19) (Fig. 5).

Findings were similar with respect to the biomodels' volume, where alterations were progressively smaller as infill percentages increased. The smallest volume alteration was observed in group 1F, where volume increased by 0.21 cm³ (SD 0.58). This alteration did not reach statistical significance (*p* value = 0.37) (Fig. 6).

The volume of the original 3D image prior to printing was 15.805 cm³, while the original area was 38.146 cm². The mean area of the biomodel after undergoing printing

and scanning (prior to sterilization) was 37.57 cm², while its volume was 15.65 cm³. As a result of printing and scanning, the biomodel lost 0.15 cm² (i.e., 1%) of its area volume. As regards volume area, the loss observed was 0.57 cm³, i.e., 3.6%. Prior to sterilization, there were no statistically significant differences between the groups in terms of the volumes or the areas of the biomodels printed (*p* value < 0.01), which means that the printing and scanning error remained constant across all the groups.

The mean number of surface points of the biomodel compared in each analysis was 376,732.60.

All cultures from group 2B (*n* = 62) exhibited monomicrobial growth compatible with the previously cultured pathogen, which was indicative of the absence of contamination and the effectiveness of the inoculation method employed. Staining in group 2C (*n* = 62) demonstrated biofilm formation across all biomodels, which attested to the correctness of the inoculation process.

Following sterilization, no pathogen growth was observed in group 2A (*n* = 62) during the observation process, demonstrating 100% effectiveness of the sterilization process. Negative controls (*n* = 6) did not exhibit signs of growth and biofilm staining was negative.

Discussion

Hospital-FFF manufactured 3D biomodels with PLA filaments may be effectively sterilized without significantly altering their morphology by means of conventional autoclaving. To be successful, it is essential to follow the protocol proposed in Table 2 as well as an infill percentage lower than 25%, which will lead to a mean deformation of approximately 0.14 mm with a sterilization success rate of nearly 100%.

One of the areas where 3D has shown the greatest promise is that of preoperative planning for fractures [23–25].

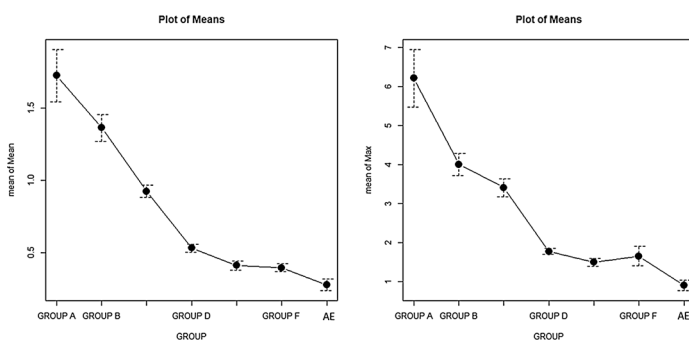
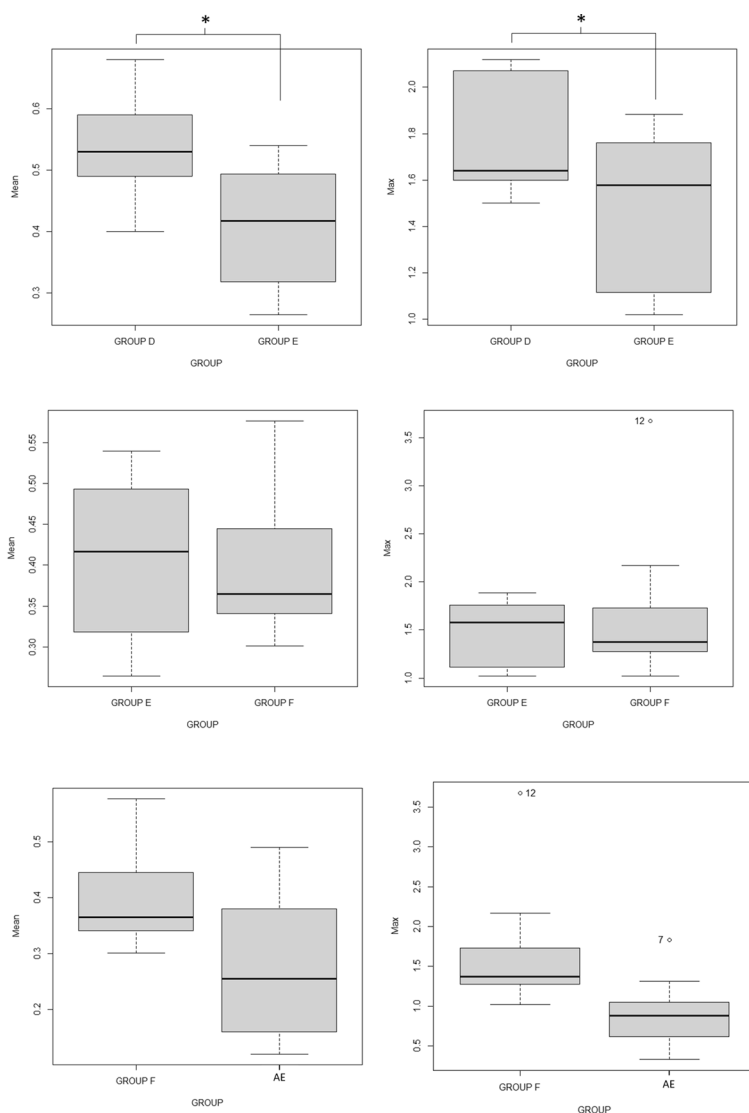


Fig. 3 Diagram showing the mean and maximum autoclaving-induced deformation. *Statistically significant differences ($\alpha < 0.01$)

GROUP	Max difference	Mean difference
GROUP 1A	6.21 (SD 2.33)	1.72 (SD 0.57)
GROUP 1B	4 (SD 0.89)	1.36 (SD 0.29)
GROUP 1C	3.41 (SD 0.72)	0.92 (SD 0.12)
GROUP 1D	1.77 (SD 0.24)	0.53 (SD 0.08)
GROUP 1E	1.49 (SD 0.32)	0.41 (SD 0.09)
GROUP 1F	1.65 (SD 0.78)	0.39 (SD 0.08)
Alignment error (AE)	0.90 (SD 0.42)	0.27 (SD 0.12)



	GROUP 1D	GROUP 1E	P value	GROUP 1F	P value	Alignment error (AE)	P value
Mean of the differences	0.53	0.41	0.007* (0,036 - 0.2)	0.39	0.7 IC 95% (-0.06 - 0.09)	0.27	0.02 IC 95% (0.016 - 0.22)
Mean of the max difference	1.77	1.49	0.004* IC 95% (0,007 - 0.54)	1.65	0.56 IC 95% (-0.73 - 0.42)	0.9	0.01 IC 95% (0.14 - 1.35)

Fig. 4 Box diagram showing mean and maximum deformity values between groups. *Statistically significant differences ($\alpha < 0.01$)

Indeed, these injuries must be treated urgently, which often precludes the use of commercially manufactured biomodels. For that reason, to be able to correctly plan for fracture surgery using 3D biomodels hospitals must be autonomous in the production of such models.

Following the expiry of patent number US5121329A, which belonged to Stratasys until 30 October 2009, FFF became much more economical and therefore accessible to most hospitals for the manufacture of 3D biomodels.

Autoclaving being the most widely used method for sterilization worldwide, Boursier et al. analyzed the effect of autoclave temperature on the sterilization of FFF printed objects with PLA filaments, obtaining minimum deformation values [26]. However, the authors did not evaluate the effectiveness of the sterilization process or defined the printing parameters they used [26].

Other authors have looked at the effects of autoclave sterilization on the strength of 3D printed models [17, 27–29]

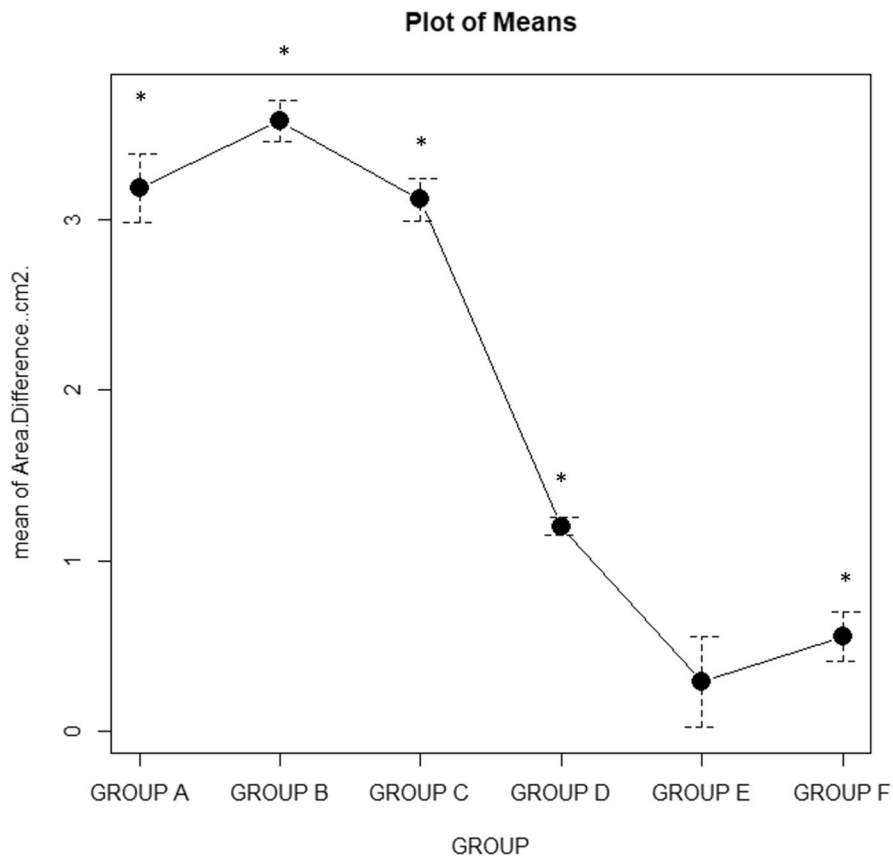


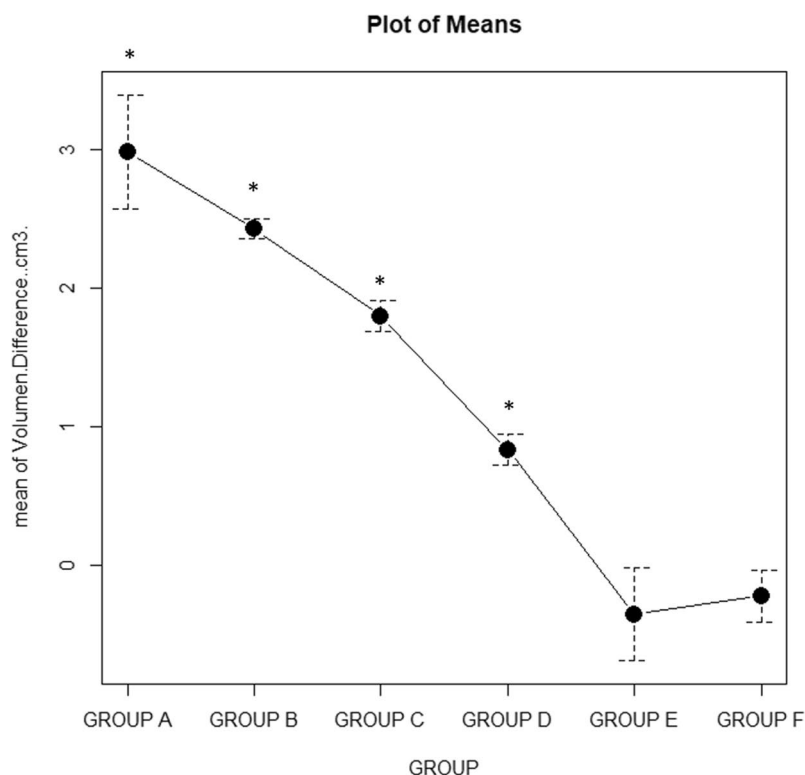
Fig. 5 Mean values of the groups, showing the area changes that occurred following autoclave sterilization. In group E, the pre- and post-sterilization area difference was not statistically significant

in an attempt to evaluate the capabilities of 3D printing for the manufacturing of surgical instruments [30]. Nonetheless, few studies have analyzed morphological changes, which are much more important than strength for the generation of biomodels.

3D printed biomodels are considered a custom-made medical product and, in accordance with article 30 of European Act 5.5.2017, hospitals are allowed to manufacture these products for non-commercial purposes. The main barrier to the widespread implementation of 3D models in

hospitals is not of a legal nature but, rather, it is related to the steep learning curve and the safe printing protocols required.

One of the main contributions of this study is that it proposes a safe, affordable, and reproducible 3D printing protocol (Table 2). Given the availability of an open-access software package compatible with the vast majority of present-day 3D printers like Cura, this protocol can be applied in virtually any hospital in the world, with very basic or highly sophisticated 3D printers, to print 3D biomodels during the preoperative planning in most of the fractured bones.



GROUP	Pre-sterilization	Post-sterilization	Mean of the differences	P value
GROUP 1A	15.79 (SD 0.32)	12.81 (SD 1.16)	2.98 (SD 1.3)	< 0.01*
GROUP 1B	15.63 (SD 0.09)	13.20 (SD 0.16)	2.42 (SD 0.23)	< 0.01*
GROUP 1C	15.66 (SD 0.14)	13.87 (SD 0.3)	1.79 (SD 0.35)	< 0.01*
GROUP 1D	15.89 (SD 0.13)	15.06 (SD 0.38)	0.83 (SD 0.35)	< 0.01*
GROUP 1E	15.57 (SD 0.24)	15.92 (SD 1.08)	-0.34 (SD 1.05)	0.19
GROUP 1F	15.36 (SD 0.28)	15.58 (SD 0.46)	-0.21 (SD 0.58)	0.37

Fig. 6 Mean values of the groups, showing the volume changes that occurred following autoclave sterilization. In groups E and F, the pre- and post-sterilization volume difference was not statistically significant

The main limitation of the present study is that it only focuses on one parameter, namely infill percentage, of the many that can be configured to increase the thermal resistance of biomodels. In some cases, a lower infill percentage could be adequate if, for example, the number of external layers or the wall thickness were greater, specially in small bones whereby the infill area is very small. The reason why we focused on infill percentage rather than on some other parameter had to do with the fact that infill is the main contributor to mechanical strength in large objects like biomodels, whereas wall thickness is a more important factor for

smaller objects. The infill pattern is another important key part in the 3D printed biomodels and the optimal printing protocol could be quite different using other infill pattern. In our study, we selected the gyroid pattern due to its lightweight and our experience with it, but other infill patterns can be as useful as gyroid pattern with an adequate printing protocol. Future studies should analyze combinations of different parameters with a view to increasing thermal resistance. The protocol presented here is an effective alternative but by no means the only one. However, it is probably the most effective alternative so far reported in the literature.

Another important limitation of our study is that only one kind of filament was used. The properties of the filament may be slightly different across manufacturers. The thermal plasticity properties provided by the different manufacturers should be compared to determine the relevance of this aspect. The reason why we focused our analysis on the PLA filament is that it is economical and easily accessible. Moreover, the biomodel used for the study was a normal distal radius. Morphometric analyses of other body parts could yield slightly different results. In an attempt to overcome this problem, we have expressed the area and volume changes in terms of total initial area and volume values.

Conclusions

The protocol proposed in the present study makes it possible for any hospital to access the benefits offered by the technology discussed. The study provides a series of guidelines on how hospitals should go about the printing work, enhancing their autonomy and performing their preoperative planning using 3D models to speed up the recovery of their patients.

Authors contributions JF-T: Development of the idea and 3D-printed samples. OS-B: Cultures and sterilization evaluation. JMS-A: Cultures and sterilization evaluation. MA-S: Statistical analyses. CDC: Evaluation of the results and critical analysis. JVA-V: Evaluation of the results and critical analysis. FB-G: Biomechanical analysis.

Funding This study was funded by a grant from the Spanish Society of Orthopedic and Trauma Surgery (Grant number 2020/1).

Declarations

Conflict of interest The authors declare they have no conflict of interest with respect to the present study.

References

- Tack P, Victor J, Gemmel P, Annemans L. 3D-printing techniques in a medical setting: a systematic literature review. *Biomed Eng Online*. 2016;15(1):115.
- Auricchio F, Marconi S. 3D printing: clinical applications in orthopaedics and traumatology. *EFORT Open Reviews*. 2016;1(5):121–7.
- Vaishya R, Patralekh MK, Vaish A, Agarwal AK, Vijay V. Publication trends and knowledge mapping in 3D printing in orthopaedics. *J Clin Orthop Trauma*. 2018;9(3):194–201.
- Wong KC, Kumta SM, Geel NV, Demol J. One-step reconstruction with a 3D-printed, biomechanically evaluated custom implant after complex pelvic tumor resection. *Computer Aided Surg*. 2015;20(1):14–23 (New York, NY).
- Bizzotto N, Tami I, Santucci A, Adani R, Poggi P, Romani D, et al. 3D printed replica of articular fractures for surgical planning and patient consent: a two years multi-centric experience. *3D Print Med*. 2016;2(1):1–6.
- Zheng W, Su J, Cai L, Lou Y, Wang J, Guo X, et al. Application of 3D-printing technology in the treatment of humeral intercondylar fractures. *Orthop Traumatol Surg Res*. 2018;104(1):83–8.
- Wang Q, Hu J, Guan J, Chen Y, Wang L. Proximal third humeral shaft fractures fixed with long helical PHILOS plates in elderly patients: benefit of pre-contouring plates on a 3D-printed model—a retrospective study. *J Orthop Surg Res*. 2018;13(1):203.
- Xie L, Chen C, Zhang Y, Zheng W, Chen H, Cai L. Three-dimensional printing assisted ORIF versus conventional ORIF for tibial plateau fractures: a systematic review and meta-analysis. *Int J Surg*. 2018;57:35–44.
- Ferràs-Tarragó J, Sanchis-Alfonso V, Ramírez-Fuentes C, Roselló-Añón A, Baixauli-García F. A 3D-CT analysis of femoral symmetry—surgical implications. *J Clin Med*. 2020;9(11):3546.
- Ferràs-Tarragó J, Sanchis-Alfonso V, Ramírez-Fuentes C, Roselló-Añón A, Baixauli-García F. Locating the origin of femoral malrotation using 3D volumetric technology—the Hockey stick theory. *J Clin Med*. 2020;9(12):3835.
- Schubert C, van Langeveld MC, Donoso LA. Innovations in 3D printing: a 3D overview from optics to organs. *Br J Ophthalmol*. 2014;98(2):159–61.
- Liu S, Wu G, Chen X, Zhang X, Yu J, Liu M, et al. Degradation behavior in vitro of carbon nanotubes (CNTs)/poly(lactic acid) (PLA) composite suture. *Polymers*. 2019;11(6):1015.
- Singhvi MS, Zinjarde SS, Gokhale DV. Polylactic acid: synthesis and biomedical applications. *J Appl Microbiol*. 2019;127(6):1612–26.
- Liu S, Yu J, Li H, Wang K, Wu G, Wang B, et al. Controllable drug release behavior of polylactic acid (PLA) surgical suture coating with ciprofloxacin (CPFX)-polycaprolactone (PCL)/polyglycolide (PGA). *Polymers*. 2020;12(2):288.
- Tyler B, Gullotti D, Mangraviti A, Utsuki T, Brem H. Polylactic acid (PLA) controlled delivery carriers for biomedical applications. *Adv Drug Deliv Rev*. 2016;107:163–75.
- Shintani H. Ethylene oxide gas sterilization of medical devices. *Biocontrol Sci*. 2017;22(1):1–16.
- Shaheen E, Alhelwani A, Van De Castele E, Politis C, Jacobs R. Evaluation of dimensional changes of 3D printed models after sterilization: a pilot study. *Open Dent J*. 2018;12(1):72–9.
- Zhao Y, Zhu B, Wang Y, Liu C, Shen C. Effect of different sterilization methods on the properties of commercial biodegradable polyesters for single-use, disposable medical devices. *Mater Sci Eng C*. 2019;105:110041.
- Savaris M, Santos VD, Brandalise RN. Influence of different sterilization processes on the properties of commercial poly(lactic acid). *Mater Sci Eng C*. 2016;69:661–7.
- Aguado-Maestro I, De Frutos-Serna M, González-Nava A, Merino-De Santos AB, García-Alonso M. Are the common sterilization methods completely effective for our in-house 3D printed biomodels and surgical guides? *Injury* 2020
- Cignoni P, Callieri M, Corsini M, Dellepiane M, Ganovelli F, Ranzuglia G. MeshLab: an open-source mesh processing tool. 2008. Available at: <https://search.datacite.org/works/https://doi.org/10.2312/localchapterevents/italchap/italianchapconf2008/129-136>.
- Cignoni P, Callieri M, Corsini M, Dellepiane M, Ganovelli F, Ranzuglia G. MeshLab: an open-source mesh processing tool. In: *Eurographics Italian Chapter Conference 2008*, pp. 129–136 (2008).
- Foo GL, Kwek EBK. Are three-dimensional printed models useful for preoperative planning of tibial plafond fractures? *J Foot Ankle Surg*. 2019;58(4):723–729.
- Xiong L, Li X, Li H, Chen Z, Xiao T. The efficacy of 3D printing-assisted surgery for traumatic fracture: a meta-analysis. *Postgrad Med J*. 2019;95(1126):414–9.

25. Kang HJ, Kim BS, Kim SM, Kim YM, Kim HN, Park JY, et al. Can preoperative 3D printing change surgeon's operative plan for distal tibia fracture? *Biomed Res Int*. 2019;2019:1–7.
26. Boursier J, Fournet A, Bassanino J, Manassero M, Bedu A, Leperlier D. Reproducibility, accuracy and effect of autoclave sterilization on a thermoplastic three-dimensional model printed by a desktop fused deposition modelling three-dimensional printer. *Vet Comparative Orthop Traumatol*. 2018;31(6):422–30.
27. Standau T, Long H, Murillo Castellón S, Brütting C, Bonten C, Altstädt V. Evaluation of the zero shear viscosity, the D-content and processing conditions as foam relevant parameters for autoclave foaming of standard polylactide (PLA). *Materials*. 2020;13(6):1371.
28. Zolfagharian A, Khosravani MR, Kaynak A. Fracture resistance analysis of 3D-printed polymers. *Polymers*. 2020;12(2):302.
29. Török G, Gombocz P, Bognár E, Nagy P, Dinya E, Kispélyi B, et al. Effects of disinfection and sterilization on the dimensional changes and mechanical properties of 3D printed surgical guides for implant therapy—pilot study. *BMC Oral Health*. 2020;20(1):19.
30. Ferràs-Tarragó J, Jordà-Gómez P, Català-de-las-Marinas J, Antequera-Cano JM, Barrés-Carsí M. A new universal 3D-printable device to prevent excessive drilling in orthopedic surgery. *Euro J Trauma Emergency Surgery*. 2020. <https://doi.org/10.1007/s00068-020-01465-3>.